Laser-induced surface modification of biopolymers – micro/nanostructuring and functionalization

IOP Conf. Series: Journal of Physics: Conf. Series **992** (2018) 012051 doi:10.1088/1742-6596/992/1/012051

Laser-induced surface modification of biopolymers – micro/nanostructuring and functionalization

N E Stankova[1,6], P A Atanasov[1], N N Nedyalkov[1], Dr Tatchev[2], K N Kolev[2], E I Valova[2], St A Armyanov[2], K Grochowska[3], G Śliwiński[3], N Fukata[4], D Hirsch[5] and B Rauschenbach[5]

[1]E. Djakov Institute of Electronics, Bulgarian Academy of Sciences, 72 Tzarigradsko Chaussee, 1784 Sofia, Bulgaria
[2]Acad. R. Kaishev Institute of Physical Chemistry, Bulgarian Academy of Sciences, Acad. G. Bonchev Str., Bl. 11, 1113 Sofia, Bulgaria
[3]Photophysics Department, The Szewalski Institute, Polish Academy of Sciences, 14 Fiszera Str., 80-231 Gdańsk, Poland
[4]International Center for Materials for NanoArchitectonics (MANA), National Institute for Materials Science (NIMS), 1-1Namiki, Tsikuba 305-0044, Japan
[5]Leibniz Institute of Surface Modification (IOM), 15 Permosestrasse, D-04318 Leipzig, Germany

E-mail: nestankova @yahoo.com

Abstract. The medical-grade polydimethylsiloxane (PDMS) elastomer is a widely used biomaterial in medicine for preparation of high-tech devices because of its remarkable properties. In this paper, we present experimental results on surface modification of PDMS elastomer by using ultraviolet, visible, and near-infrared ns-laser system and investigation of the chemical composition and the morphological structure inside the treated area in dependence on the processing parameters – wavelength, laser fluence and number of pulses. Remarkable chemical transformations and changes of the morphological structure were observed, resulting in the formation of a highly catalytically active surface, which was successfully functionalized via electroless Ni and Pt deposition by a sensitizing-activation free process.

The results obtained are very promising in view of applying the methods of laser-induced micro- and nano-structuring and activation of biopolymers' surface and further electroless metal plating to the preparation of, e.g., multielectrode arrays (MEAs) devices in neural and muscular surface interfacing implantable systems.

1. Introduction

Polydimethylsiloxane (PDMS) is medical grade silicone and is one of the most widely-used polymeric materials in biomedical implantable devices, such as substrate insulator carriers and/or for packaging of such devices [1-4]. The popularity of PDMS in such medical application is based on its distinctive characteristics, which include tensile strength, chemical and biological inertness, non-toxicity,

[6] To whom any correspondence should be addressed,

permeability to gasses, high dielectric constant and breakdown field, optical transparency in the UV, VIS and NIR spectral ranges, which determine its high biocompatible and biostable nature [4]. Owing to these advantageous properties and the simple and inexpensive fabrication process, PDMS is a suitable and preferred material for fabrication of long-term implantable devices [5]. Overall, PDMS-based elastomers are extremely stable and keep their high flexibility. They are excellent insulators and have clinical approval according to USP class VI for unrestricted use in chronic implants. Photo-detectable PDMS elastomers are also available that increase the absorption in the UV region (below 365 nm), thus improving the processing conditions under irradiation by such light sources (lasers, excimer lamps). However, they are not applicable in the implantable grades. Surface processing of PDMS elastomers is needed to improve their surface properties, like wettability or adhesion features for further functionalization, e.g., metallization. Highly-flexible polymeric multielectrode arrays (MEAs) based on PDMS-elastomer scaffolds are applied as neural interfacing technologies for monitoring and/or stimulation of neural activity by connecting the neurons to electronic circuitry [6-8]. Elastomeric MEAs can be rolled and flexed, thus offering an improved structural interface with the neural tissues. UV, VIS and NIR ns- and fs-laser processing of the PDMS elastomer is a powerful method for surface modification and activation without altering the material's bulk properties [9-18]. Generally, laser micromachining is based on direct laser ablation or surface modification for fabrication of tracks, holes and complex 2D/3D structures with dimensions of several tens of microns or less in a wide range of materials. It is a low-cost technique, unique with the versatile control of the processing parameters. This approach opens up new interesting possibilities for rapid patterning of delicate materials on micro- and nano-scale over large areas, especially of biodegradable polymers like PDMS for tissue engineering application. Selective metallization has been reported of polymers (such as polyamide, polyurethane or polydimethylsiloxane) after laser modification (chemical activation and ablation) with Cu, Ni or Pt by using electroless plating [17-20]. Since the major demands to implants are biocompatibility and biostability, Pt is the most suitable element used in metallization via electroless deposition [17, 19].

The aim of this work was to provide complex data on the modification and activation of the PDMS elastomer surface by using the traditional method of ns-laser processing followed by successful functionalization of the laser-modified surface. The effects of the laser parameters on the chemical structure and the morphology after UV, VIS and NIR treatment were studied and compared. The trenches produced were successfully metalized by Ni or Pt deposition by an improved autocatalytic coating bath – a tin- and palladium-free process. Our work can contribute to the research efforts to achieve successful direct laser writing of micro channels via ns-laser processing of polymer materials and their functionalization for application as MEAs in neural interface technologies.

2. Experimental

For surface processing of medical grade PDMS elastomers (MED 4860 and SSPM823), we used a Q-switched Nd:YAG laser multimode system oscillating at the fundamental wavelengths of 1064 nm and its harmonics: second (532 nm), third (355 nm) and fourth (266 nm), with a pulse duration of 15 ns and a repetition rate of 10 Hz. The thickness of the sheets was between 150 μm and 200 μm. The laser beam was focused normally to the sample by UV fused-silica lenses with different focal lengths (between 10 cm and 25 cm). In order to obtain a larger laser beam spot, lenses with a higher focal length combined with a homogenizer (with relevant parameters) were used. The samples were mounted on a stepper-motor computer-controlled *x-y* stage, which allowed fabrication of single trenches by overlapping 10 to 220 consecutive laser pulses. The number of pulses depended on the laser spot size on the sample surface and the stage speed of motion. The laser processing was performed in air at ambient temperature. The laser fluence was a function of the wavelength and the beam spot size. The data on the laser processing parameters are presented in table 1.

The absorption coefficient (α) and the penetration depth (δ) were calculated following the Beer-Lambert law; as the scattering is ignored, the values represent the linear absorption coefficient. After the laser treatment, the PDMS samples were successfully metallized with Ni or Pt via electroless

deposition (autocatalytic bath). The metallization was performed without chemical sensitization by Sn and activation by Pd of the laser-treated surface. The electroless plating process is based on a hydrazine hydrate reducer at different concentrations used to increase the active sites without electrochemical methods. The details of this procedure will be described in a forthcoming communication. It should be emphasized that the electroless Ni deposition is the best and the cheapest analog of the classic Pt electroless plating process.

Table 1. Summary of the laser processing parameters.

Wavelength (nm)	266	355	532	1064
Laser Fluence (J cm^{-2})	0.5 – 1.5	2.5 – 6.0	9.5 – 12.0	13.0 – 16.0
α (cm^{-1})	14.9	7.38	3.58	2.86
δ (μm)	670	1354	2794	3502

The surface topography of the samples was investigated by a VK-9700K color 3D laser microscope (KEYENCE, Japan) and scanning electron microscopy (SEM) (Hitachi SU-70 with field-emission gun) and SEM/FIB (Lyra/Tescan dual-beam system); the structure modifications were analyzed by a μ-Raman spectrometer (Invia, Renishaw) using 514-nm excitation wavelength and beam spot on a sample ~5 μm×5 μm for a 100× objective.

3. Results and discussions

3.1. Raman spectroscopy inside the trenches

The influence of the laser radiation in the UV, VIS and NIR spectral ranges on the chemical composition of the PDMS elastomer samples was investigated by μ-Raman spectroscopy. The spectra were acquired by measuring at different points in each trench. The spectra of areas treated by different laser parameters (see Table 1) differ significantly from the spectrum of the untreated sample (figures 1 and 2). Since the PDMS elastomer belongs to the silicones' polymeric family, its backbone is composed by an alternate succession of Si–O atoms joined by a strong covalent bond of 4.7 eV. Two organic CH_3 radicals are also coupled to the Si atoms by a Si–C bond with a bond energy of 3.3 eV. The Raman peaks of native PDMS characterize the following vibration modes: 488 cm^{-1} (Si-O-Si symmetric stretching); 685 cm^{-1} (Si-CH_3 symmetric rocking); 709 cm^{-1} (Si-C symmetric stretching); 787 cm^{-1} (CH_3 asymmetric rocking + Si-C asymmetric stretching); 859 cm^{-1} (CH_3 symmetric rocking); 1262 cm^{-1} (CH_3 symmetric bending); 1411 cm^{-1} (CH_3 asymmetric bending); 2909 cm^{-1} (CH_3 symmetric stretching); and 2970 cm^{-1} (CH_3 asymmetric stretching). Obviously, the laser treatment leads to chemical modification of the PDMS surface. A typical tendency in the spectra is observed at all wavelengths applied. The intensity of the O-Si-O bond at 488 cm^{-1} decreases or almost disappears and a new sharp and strong peak appears between 515 cm^{-1} and 519 cm^{-1}. This peak is attributed to mono and/or polycrystalline or only to monocrystalline silicon (c-Si) [21]. This can be explained by chemical transformations occurring during the laser processing – breaking of the O-Si-O bonds and formation of crystalline Si as a result of the higher pressure and temperature in the laser spot area. It is worth noting that the intensity of the other peaks of the native PDMS elastomer decreases. This indicates that the Si-CH_3, CH_3, and Si-C bonds are also broken and probably contribute to the c-Si formation. The comparison of the spectra of trenches obtained at different processing parameters show complex dependence on the wavelength, laser fluence and number of pulses. At the wavelengths of 266 nm and 355 nm and low fluences, the c-Si peak appears after 110 or more pulses, but its intensity is still weak. As the laser fluence increases, the O-Si-O peak's intensity is reduced, while the intensity of c-Si peak is strongly enhanced. Also, this peak becomes very intensive and sharp even at low number of pulses (5-18) when higher fluences are applied. This tendency is also observed at the wavelengths of 532 nm and 1064 nm (figure 2); however, the fluence values needed to break the Si-O-Si bond significantly increase compared with the UV wavelengths (between 9.5 J cm^{-2} and 12 J cm^{-2} for 532 nm, and between 13 J cm^{-2} and 16 J.cm^{-2} for 1064 nm) at number of pulses

between 11 and 33. The chemical transformations observed after UV laser irradiation is in accordance with the known data of the photon energy of 4.7 eV for the wavelength of 266 nm (and probably 3.5 eV for 355 nm), which is needed for the direct breaking of the covalent bonds, like Si-O-Si (4.7 eV), and/or C-H (4.3 eV), and/or S-C (3.3 eV), respectively. Probably, photochemical dissociation of the covalent bonds can take place during laser irradiation at the wavelength of 266 nm. However, at the longer wavelengths (355 nm, 532 nm and 1064 nm), the photon energy (3.5 eV, 2.3 eV and 1.2 eV, respectively), is not sufficient to cause photochemical dissociation, especially for the Si-O-Si bond. Therefore, the chemical decomposition observed can rather be the result of heat accumulated with each subsequent pulse per unit area. In the current experiments on ns-laser irradiation of the PDMS polymer, the ablation mechanism can be due predominantly to the thermal (vibrational) relaxation of the excited states, especially at the wavelength of 355 nm and longer. It can also be assumed that during the ultraviolet irradiation at 266 nm, photothermic reactions contribute to the mechanism of ablation simultaneously with the photochemical reactions. The ratio between them depends both on the laser parameters and the properties of the polymer. In summary, all μ-Raman spectra provide evidence that the PDMS elastomer surface is chemically transformed and activated after ns-laser processing.

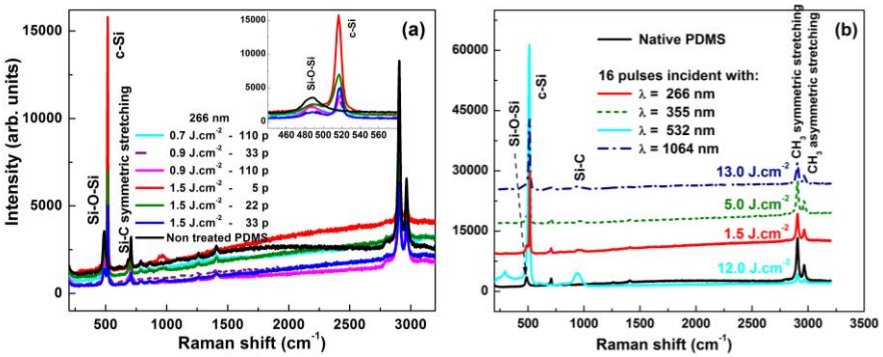

Figure 1. μ-Raman spectra of native (non-treated) and ns-laser treated PDMS elastomer at: a) 266 nm; b) comparison between treatment at 266, 355, 532 and 1064 nm.

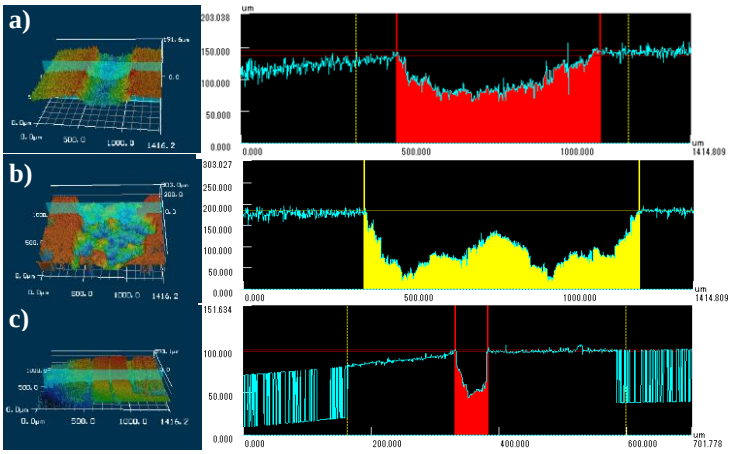

Figure 2. Laser microscope images - photographs and profiles: a) 266 nm, 0.5 J cm^{-2} and N=22 pulses; b) 1064 nm, 13 J cm^{-2} and N=22 pulses; c) U-shaped high definition track produced at 266 nm, 1.5 J cm^{-2} and 44 pulses.

3.2. Laser microscope views of the trenches

The quality of the profiles of the laser-produced trenches was viewed and assessed by 3D color laser microscopy (figure 2). Since the laser system emits a multimode beam, the profiles of trenches are generally inhomogeneous, especially in the cases of VIS and NIR irradiation and/or higher number of pulses. This is due to the inhomogeneous distribution of the energy density inside the laser beam, namely, the existence of "hot" spots in the beam structure. However, in a dynamic mode of laser processing, where the overlapping of the consecutive pulses is controlled by varying the *x*-*y* table speed of motion, one can produce trenches with homogeneous profiles owing to the processing equalization after a large number of pulses are applied per unit area. The UV laser treatment results in

highly homogeneous profiles (mainly at 266 nm) regardless of the number of pulses and the laser spot size on the surface. This is due to the higher absorption coefficient (i.e., the short penetration depth at this wavelength) of the PDMS polymer, which for 266 nm is an order of magnitude higher than those for the wavelengths of 355 nm, 532 nm, and 1064 nm (see table 1). Using irradiation at the wavelength of 266 nm, we were able to produce high-definition U-shaped or straight-line laser tracks.

3.3. Scanning electron microscope views of the trenches – after laser processing and after electroless metal deposition

Typical SEM images of the trenches produced after ns-laser processing of the PDMS elastomer are presented in figure 3. The surface morphology is significantly modified compared to the non-treated surface due to the local laser ablation. The SEM analysis shows formation of similar morphologic structures at all wavelengths used. An extremely developed relief with a cauliflower-like structure is formed on a micro-scale, which can ensure good adhesion of the metal coating. In general, the ablation depth increases with the laser fluence and/or the number of the pulses. As it is seen, cavities of different size are formed in all cases. However, they become larger at VIS and NIR irradiation or as the laser exposure of the sample is increased at a given wavelength. The high-resolution images indicate that the modified surface is nanostructured with a granular chondrites-like structure.

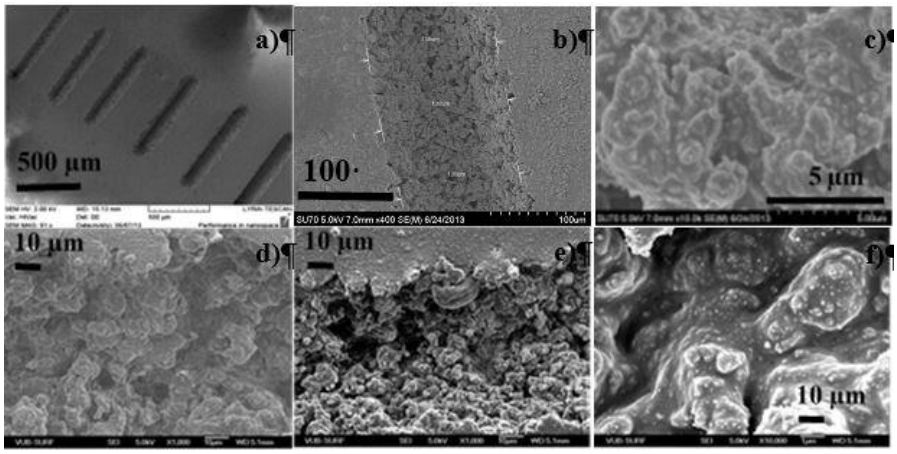

Figure 3. Trenches produced by ns-laser: **a)** 355 nm, N=11, 22, 33, 44, 55 and 110 pulses, respectively, and 4 J cm^{-2}; **b)** 266 nm, N=55 and 1.5 J cm^{-2}; **c)** HR SEM of b); **d)** 532 nm, N=16 and 9.5 J cm^{-2}; **e)** 1064 nm, N=16 and 13 J cm^{-2}; **f)** HR SEM of e).

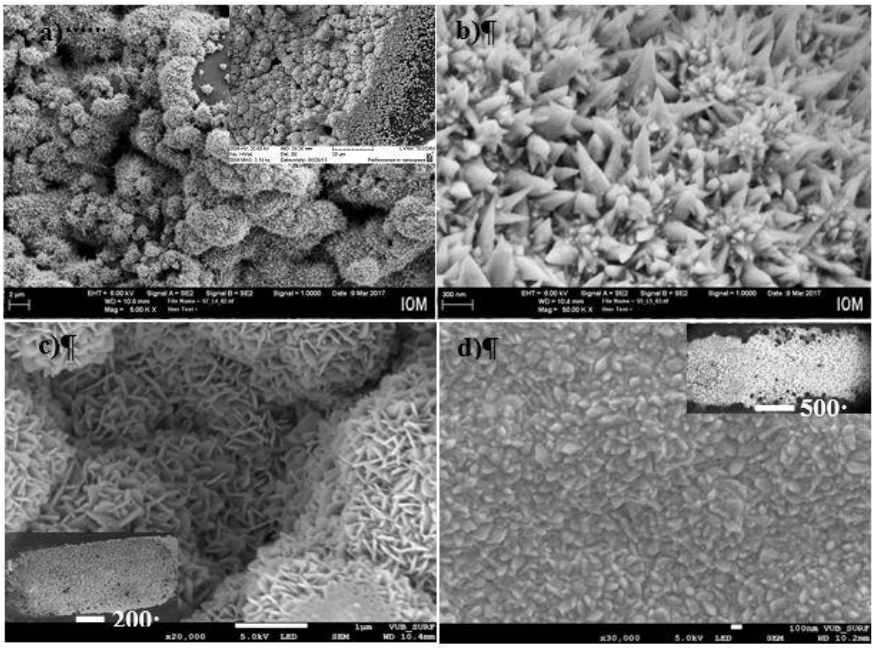

Figure 4. SEM images of the metal nanospike structures after electroless coating of the trenches produced at: a) 266 nm – Ni metallized; b) HR SEM of a); c) 266 nm and d) 355 nm after Pt metallization in HR mode. The inset images show whole (c) and d)) or part (a)) of the trenches.

The laser-modified and thus activated surface of the PDMS elastomer samples ensured their successful functionalization by electroless deposition of Ni or Pt metals. The metallization was successfully performed regardless of the time-interval between the laser exposure and the autocatalytic bath. Figure 4 shows SEM images of electroless deposited Ni (figure 4a) and 4b)) and Pt (figure 4c) and 4d)) films. Metal crystallites with a "spiky" structure were uniformly deposited on the laser-treated areas. The metal nanospikes tended to grow vertically with size ranging from several tens to several hundreds of nanometers. Since the hydrazine was used as a reductant in the autocatalytic bath, the deposition of Ni and Pt resulted in the formation of nanospike arrays. Depending on the hydrazine concentrations, some small differences in the crystallites structure could be found, but the "spiky" origin remained.

4. Conclusions

The results obtained in our study of laser-induced surface modification of the PDMS elastomer and its further functionalization can be summarized as follows: i) ns-lasers, generating in the UV, VIS and NIR spectra are effective tools for micro- and nanostructuring and chemical activation of biopolymeric elastomers: (1) a significant increase of the surface roughness by laser ablation, which results in the formation of trenches with controllable size depending on the laser beam parameters and (2) chemical activation of the laser-processed area by breaking the covalent bonds (Si-O-Si, Si-C) of the PDMS polymer and formation of Si micro-crystallites; ii) successful metallization of the ns-laser treated PDMS elastomer surface via Pt and Ni electroless plating: (1) excluding Sn sensitization and Pd activation by using hydrazine hydrate as catalyst and (2) growth of Pt and Ni nanospike-structured arrays on a nanometer scale.

The results reported describe a simple procedure of biopolymer surface preparation for its following functionalization, which opens up new possibilities for rapid prototyping of micro- and nano-structures suitable for various applications, such as MEAs in neural implants interfacing technologies.

References

[1] Hassler C, Boretius T and Stieglitz T 2011 *J. Polym. Sci.* B*: Polym. Phys*. **49**/1 18
[2] Liang G, Guvanasen G S, Xi L,Tuthill C, Nichols T R and De Weerth S P 2013 *IEEE Trans. Biomed. Circuitsand Syst.***7**/1 1
[3] Adrian J, Teo T, Mishra A, Park I, Kim Y-J, Park W-T and Yoon Y-J 2016 *ACS Biomater. Sci. Eng.* **2**/4 454
[4] Stieglitz T and Meyer J-U 2006 *BIOMEMS* ed Urban G A (Springer: Dordrecht, The Netherlands) **3** 41
[5] Curtis J M and Colas A 2004 Dow Corning (R) Silicone biomaterials: history, chemistry & medical applications of silicones *Biomaterials Science 2nd Edition*; ed Ratner B D (Elsevier: London)
[6] Hassan H M, Chodavarapu V and Musallam S 2008 *Review: NeuroMEMS: Neural Probe Microtechnol., Sensors* **8**/10 6704
[7] Lacour S, Benmerah S, Tarte E, Gerald J F, Serra J, Mc Mahon S, Fawcett J, Graudejus O, Yu Z and Morrison B 2010 *Med. Biol. Eng. Comput*. **48**/10 945
[8] Liang G, Guvanasen G S , Xi L, Tuthill C, Nichols T R and DeWeerth S P 2013 *IEEE Trans. Biomed. Circuits Syst.* **7**/1 1
[9] Deepak K L N, Venugopal Rao S and Narayana Rao D 2010 *J. Phys.* **75**/6 1221
[10] Dicara Cl, Robert T, Kolev K, Dupas-Bruzek C and Laude L D 2003 *Proc. SPIE* **5147** 255
[11] Graubner V-M, Nuyken O, Lippert Th, Wokaun A, Lazare S and Servant L 2006 *Appl. Surf. Sci.* **252**/13 4781
[12] Dupas-Bruzek C, Robbe O, Addad A, Turrell S and Derozier D 2009 *Appl. Surf. Sci.* **255**/21 8715
[13] Van Pelt S, Frijns A, Mandamparambil R and Den Toonder J 2014 *Appl. Surf. Sci.* **303** 456

[14] Darvishi S, Cubaud T and Longtin J P 2012 *Opt. Lasers Eng.* **50** 210
[15] Sones C L, Katis I N, Mills B, Feinaeugle M, Mosayyebi A, Butement J and Eason R W 2014 *Appl. Surf. Sci.* **298** 125
[16] Surdo S, Piazza S, Ceseracciu L, Diaspro A and Duocastella M 2016 *Appl. Sur. Sci.* **374** 151
[17] Stankova N E, Atanasov P A, Nedyalkov N N, Stoyanchov T R, Kolev K N, Valova E I, Georgieva J S, Armyanov St A, Amoruso S, Wang X, Bruzzese R, Grochowska K, Śliwiński G, Baert K, Hubin A and Delplancke M P 2015 *Appl. Surf. Sci.* **336** 321
[18] Atanasov P A, Stankova N E, Nedyalkov N N, Fukata N, Hirsch D, Rauschenbach B, Amoruso S, Wang X, Kolev K N, Valova E I, Georgieva J S and Armyanov St A 2016 *Appl. Surf. Sci.* **374** 229
[19] Dupas-Bruzek C, Drean P and Derozier D 2009 *J. Appl. Phys.* **106** 074913
[20] Rytlewski P and Żenkiewicz M 2013 *JAMME* **57**/2 59
[21] Palma C, Rossi M C, Sapia C and Bemporad E 1999 *Appl. Surf. Sci.* **138–139** 24